

3D MODEL OF PLATFORM FOR SPINNING PILOTS UNDER AN ANGLE AND OTHER MEDICAL USES

Tsvetan Kachamachkov

Technical University of Sofia, Bulgaria
Postal Sofia - 1309, „Sv. Troitsa” 303 - B - 39

Abstract

With the obtained surface registration, statistical morphometric analysis based on the coordinates' deviation can be performed. Using the two-sample Hotelling's T-squared test, the p-value at each vertex on the surface is found.

1. INTRODUCTION

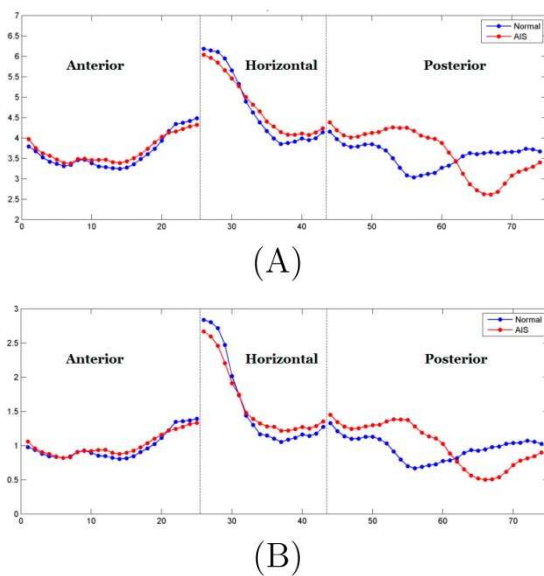


Figure 1: (A) Perimeters of each homotopic loops of the normal mean VS and the AIS mean VS. (B) Area of each minimal surfaces enclosed by the homotopic loops of the normal mean VS and the AIS mean VS.

VS is a key organ for maintaining postural balance in humans and poor postural balance is a recognized characteristic in AIS patients [1, 2]. The shape of the VS is confirmed being related to the growth of vertebrates.

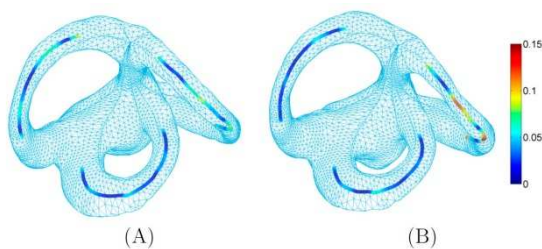


Figure 2: (A) mean surface of normal subjects. (B) mean surface for AIS subjects. Distances of each points on the center lines from the best fit planes of the normal mean VS surface and AIS mean VS surface.

The distance is visualized by the color maps. Red color indicates a large deviation from the best fit plane. Lambert et al. [3] made use of frog models for experiment to conclude that asymmetric vestibular inputs could lead to imbalanced growth of the spine.

Thus, the studies on the relationship between AIS and VS abnormality become important to the etiology of the disease. Our proposed methods focus on the accurate registration and the quantitative shape analysis of the canals in the VS. Furthermore, it is also observed that there are distortions of the plane of PSC in the AIS patients. Such planar deflection was found affecting the locomotion in primates by [4]. The proposed surface registration method is shown to be helpful in the shape analysis of the complex geometry of VS. It is hoped that a standardized assessment could set out for clinical diagnosis. To examine the accuracy and stability of the measurement, a larger sample size would be included in the continuation of this study. To perform a more comprehensive local shape analysis, a complete shape index defined by the Beltrami coefficients and curvature scan be used. The shape index effectively measures the geometric difference between two VS surfaces at each vertex of surfaces. To test our proposed algorithms, experiments have been carried out to register VS surfaces of 15 normal control subjects and 12 AIS subjects. Results show that our method can effectively and accurately compute the surface registrations between the VS surfaces. Shape analysis has also been carried out using the proposed shape features and shape energy, which reveals shape differences in the posterior canal between normal and diseased AIS groups.

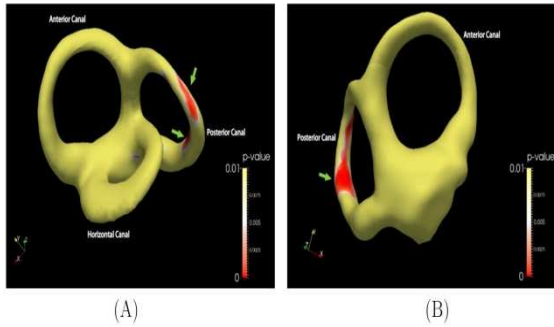


Figure 3: (A) p-map from the frontal viewpoint. (B) p-map from the backward view point. Statistical p-map showing the regions with p-value < 0:001 on the AIS mean surface (Red-colored vertex indicating p-values < 0:001).

Zero gravity has become a very popular feature among massage chair models and among massage chair shoppers. I get asked all the time about whether a particular model has zero gravity or not. Funny thing is, most folks think they want it but have no idea what it really is! But, is zero gravity something that you really want in a massage chair? I will define it and then explain to you the pros and cons of zero gravity, especially as it pertains to you, the user, and your therapeutic experience with or without it in your massage chair. In physics, zero gravity is defined, essentially, as weightlessness. However, zero gravity as it pertains to seating is defined by two conditions: 1. A 30 degree upward tilt of the seat, and 2. A 120 articulation between the tilted seat and the chair back. The essence of zero gravity in the seating paradigm is that with these angular articulations, your body and spine are not necessarily in a weightless position (because gravity is always at play here on earth!), but your body is positioned such that it's weight is evenly distributed throughout the body. Here is a great image of the Human Touch HT-7450, the first zero gravity massage chair, in its zero gravity position. Notice the upward tilt of the seat and the angle of the chair back, relative to the seat.



Figure 4: Platform for angular acceleration

2. 3D MODEL

In biology, the vestibular system is used to detect the head motion in space and results in stabilization of the visual axis, head and body posture [5]. Furthermore, the vestibular system helps with the sense for motion and change in orientation in space. The system consists of two parts: the two otolith organs (the saccule and utricle), which sense linear acceleration (gravity and translational movements), and the three semicircular canals which sense angular acceleration in three planes (pitch, roll, and yaw) [5, 6].

You are probably wondering by now what makes the angular acceleration so important, the vestibular system is affected differently by the angular acceleration this is because of the nature of the fluid in the inner ear. You are probably wondering by now what makes the angular acceleration so important, the vestibular system is affected differently by the angular acceleration this is because of the nature of the fluid in the inner ear it reacts very particular under angular acceleration this is why we have developed a new platform the platform is adaptable to all the normal system for vestibular testing usually found in hospital. One of the main strive in optimization is to accumulate a financial need for the developed product, the proper use would include usage of the already manufactured chairs for testing of the vestibular system so we focused our efforts on improving the already existing systems worldwide. We developed a unique and simple solution able to be implemented to all systems worldwide giving them the option of angular acceleration.

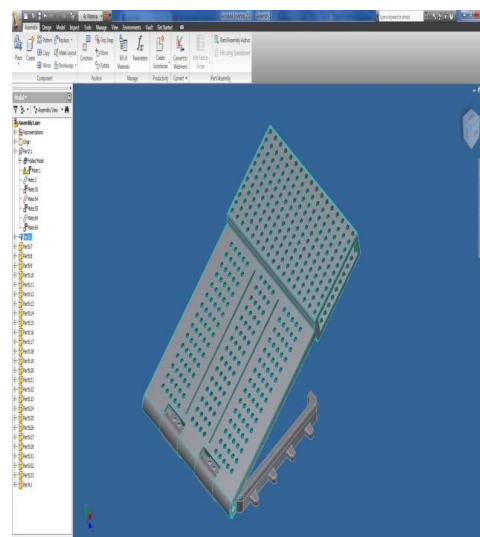


Figure 5: Platform upgrade for vestibular system experiments 3D MODEL

We are asked to compute the maximum length of a cylindrical titanium alloy specimen (before deformation) that is deformed elastically in tension. For a cylindrical specimen

$$A_0 = \pi \left(\frac{d_0}{2}\right)^2$$

where d_0 is the original diameter.

$$l_0 = \frac{\Delta l}{\varepsilon} = \frac{\Delta l}{\frac{\sigma}{E}} = \frac{\Delta l E}{\sigma} = \frac{\Delta l E}{\frac{F}{A_0}} = \frac{\Delta l E \pi \left(\frac{d_0}{2}\right)^2}{F} = \frac{\Delta l E \pi d_0^2}{4F}$$

$$= \frac{(0,42 \times 10^{-3}m) \left(107 \times \frac{10^9 N}{m^2}\right) (\pi) (3,8 \times 10^{-3})^2}{(4)(2000 N)}$$

This problem asks us to compute the diameter of a cylindrical specimen of copper in order to allow an elongation of 0.50 mm.

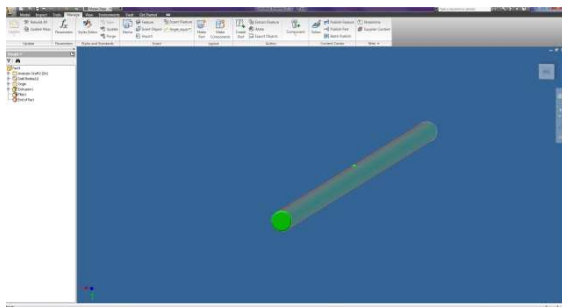


Figure 6: Mechanical analysis of the bearing axis.

The bond of the epoxy grout to the concrete foundation is stronger than the bond of the concrete to itself. Typically, concrete will separate next to the bond line of the epoxy and concrete. Therefore, the weakest link in the bond of epoxy to concrete is the concrete it self. The force required to pull concrete apart is called its shear strength. A conservative value for concrete shear strength is 800psi. To determine the force required to pullout the bolt separating it at the epoxy to concrete bond, use the following calculation strength hanch or bolt in concrete as a comparison, an anchor bolt set in a concrete foundation will typically crack up and out from the bottom of the bolt at a 45 degree angle in a cone shaped section. The force required to pull up this cone shaped section of concrete is the force required to separate concrete over the total surface area of the cone. The surface area of a

cone (sac one) = lateral surface area of a right circular cone with 45 degree sides.

PULL OUT STRENGTH IN POUNDS				
HOLE DIAMETER	BOLT LENGTH			
	3"	4"	5"	10"
5/8"	4,710	6,280	7,850	15,700
3/4"	5,650	7,530	9,420	18,840
1"	7,530	10,050	12,560	25,130
1.5"	11,309	15,070	18,840	37,690
2.0"	15,070	20,100	25,130	50,260

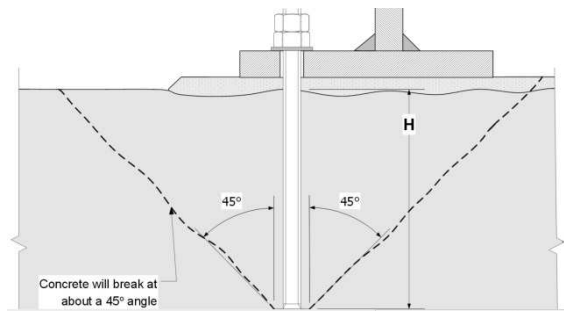


Figure 7: Acker bolts standard.

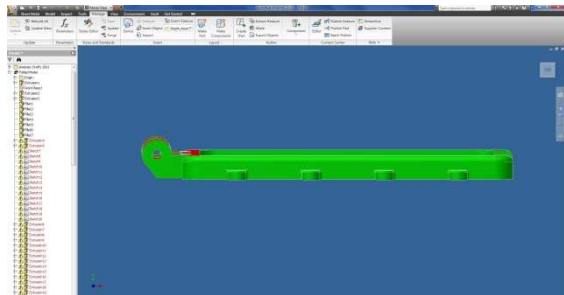


Figure 8: Mechanical analysis of the bearing fundament with anchor bolts.

CONCLUSIONS

The goal of this paper was to demonstrate that MEMS technology is a viable candidate for implementing a completely implantable vestibular prosthesis. Based on the available physiological data, we have identified performance requirements for the vestibular prosthesis and concluded that MEMS sensors can provide better performance than the human's sensation thresholds. Experimental data for a prototype of ADI's surface micromachined rate gyroscope supports the claim. Weal so presented an architecture for the vestibular prosthesis and fabricated the first prototype of the sensing unit of the prosthesis. Development of the completely implantable vestibular prosthesis is in its initial phase of exploration. Many technical issues need to be addressed, including the design of a robust low-drift sensing unit on the same chip,

design of control architecture suppressing the drift over time in the unit, integration of pulse generator and stimulator on the same chip, capability providing wireless programming and power beaming to the chip, design of bio-compatible package for the prosthesis, and interface of the prosthesis with neurons. Benefiting from the unique capabilities of the MEMS technology, this vestibular implant will be small and consume little power, and can be potentially manufactured in large quantities at low cost.

ACKNOWLEDGMENTS

The research described in this paper is supported by the Scientific Research Sector of TU-Sofia under the contract No 152пд0054-07

References

- [1] T. Haumont, G. C. Gauchard, P. Lascombes, P. P. Perrin, Postural instability in early-stage idiopathic scoliosis in adolescent girls, *Spine* 36 (13) (2011) E847{E854.
- [2] N. N. Byl, S. Holland, A. Jurek, S. S. Hu, Postural imbalance and vibratory sensitivity in patients with idiopathic scoliosis implications for treatment, *Journal of Orthopaedic & Sports Physical Therapy* 26 (2) (1997) 60{68.
- [3] F. M. Lambert, D. Malinvaud, J. Glaunes, C. Bergot, H. Straka, P. P. Vidal, Vestibular asymmetry as the cause of idiopathic scoliosis: A possible answer from xenopus, *Journal of Neuroscience* 29 (40) (2009) 12477{12483.
- [4] M. D. Malinzak, R. F. Kay, T. E. Hullar, Locomotor head movements and semicircular canal morphology in primates, *Proceedings of the National Academy of Sciences of the United States of America* 109 (44)(2012) 17914{17919.
- [5] C. Fernández and J. M. Goldberg, "Physiology of peripheral neurons innervating semicircular canals of the squirrel monkey. II. Response to sinusoidal stimulation and dynamics of peripheral vestibular system," *J. Neurophysiol.*, vol. 34, no. 4, pp. 661–675, Aug. 1971.
- [6] S. B. Yakushin, T. Raphan, J.-I. Suzuki, Y. Arai, and B. Cohen, "Dynamics and kinematics of the angular vestibulo-ocular reflex in monkey: effects of canal plugging," *J. Neurophysiol.*, vol. 80, no. 6, pp. 8077–8099, 1998.